Chaotic self-sustaining structure embedded in the turbulent-laminar interface

Toshiki Teramura[*] and Sadayoshi Toh

Department of Physics and Astronomy, Graduate School of Science, Kyoto University, Kyoto 606-8224, Japan

An interface structure between turbulence and laminar flow is investigated in two-dimensional channel flow. This spatially localized structure not only sustains itself but also converts the laminar state into turbulence actively. A filtered simulation technique is introduced to understand the invading process as an inhomogeneity-induced self-sustaining coherent structure, which consists of a meandering jet on bulk-region and near-wall vortex pairs. A phenomenological model, called the ejection-jet cycle, reveals the relationship between the spatial inner structure of the interface and the invading speed. This model gives insight on the inner-outer interaction in wall-turbulence.

Introduction. Turbulence ubiquitously appears in nature, from quark-gluon plasma [1] to the universe [2]. Because of its strong nonlinearity, most studies related to turbulence may have adopted more or less statistical or coarse-graining approaches [3]. Though they have vividly revealed phenomenological and/or kinematic natures of turbulence such as the energy transfer among different scales and places, these statistical treatments are not sufficiently adequate to elucidate concrete mechanisms of even such fundamental processes of turbulence, such as what substance, e.g., vortices, transfers energy or why the energy transfer occurs. On the other hand, the dynamical systems approaches to turbulence have helped us describe these mechanisms with numerically obtained components (invariant sets) in the phase space such as fixed points, periodic orbits, and their connections [4].

Recent developments in the dynamical systems approach to turbulence arrive at the next stage, where the spatial inhomogeneity is taken into account. Famous actors on the previous stage are the so-called minimal flows [5], which mean direct numerical simulations with minimal system sizes reproducing elementary processes and basic statistical quantities of turbulence. These studies have introduced the idea of self-sustaining coherent structures. There are several attempts to understand spatial inhomogeneity in turbulence from self-sustaining coherent structures and phenomenological interactions among them [6,7]. This approach has succeeded in flows at low Reynolds number, where vortex structures are similar to those appearing in minimal flows. However, experiments and numerical simulations suggest different types of coherent structures live together in flows at high Reynolds number [8,9]. We present a simple example in which two dynamically coupled different coherent structures of different scales coexist.

We focus on interfaces which have critical importance to understand inhomogeneous systems since most properties change along it. However, interfaces themselves can be complicated in a strongly nonlinear inhomogeneous state. Turbulence-laminar interface appears in many flows, e.g., boundary layers, jet, wake, and so on. In three-dimensional flows, the dynamics of the interface is spatiotemporally chaotic [10]. It is sometimes even hard to detect such

interfaces since they have intricate spatial geometries. These complexities prevent us from detailed studies of interfaces. To avoid this problem, we use a two-dimensional channel flow, where the activities of interfaces are limited compared to those in three-dimensional flows. This will be one of the simplest examples of localized chaotic coherent structures induced by spatial inhomogeneity.

In this paper, we describe the simulation setting and show an energy balance analysis. It is used to define a coherent structure, which we call chaotic interface (CI). Next, we confirm the self-sustainability of the chaotic interface using so-called filtered simulations. Here we propose a self-sustaining mechanism of the chaotic interface, called the ejection-jet cycle. A mechanism of determining the traveling speed of the interface is also argued. Finally, we discuss how our result could extend the dynamical systems approach to the inhomogeneous turbulence.

Chaotic interface structure. Two-dimensional (2D) laminar channel flow has the same critical Reynolds number Re_c as the three-dimensional one. In the 2D case, the Tollmien-Schlichting (TS) wave solution appearing at this critical point bifurcates into a weak chaotic state, which we call the chaotic TS wave, as its Reynolds number increases [11–14]. In this paper, we consider a channel which contains both turbulent and laminar regions.

We adopt a frame of reference moving at a speed c_I against the laboratory frame for CI not to march, and call it the interface frame. The streamwise and the wall-normal coordinates are denoted by x and y, respectively, in this interface frame, and this system is nondimensionalized by the half width of the channel, so that $y \in [-1,1]$. The velocity field in this frame is denoted by $\boldsymbol{u}$. We deal with a very long box $[0,L = 20\pi] \times [-1,1]$ to emulate the dynamics realized in an infinitely long channel. To clarify the direction we call the left side of Fig. 1 the turbulent side and the right side the laminar side. Since the walls move in the interface frame, the nonslip boundary conditions become $\boldsymbol{u}(x,\pm1) = -c_I\hat{\boldsymbol{x}}$, where $\hat{\boldsymbol{x}}$ denotes the x-directional unit vector. The Reynolds number Re is fixed to 8 000 in this paper to exceed the critical value $\mathrm{Re}_c = 5\,772$ of stability of the laminar flow. We have confirmed that the qualitative nature of CI reported below does not change for $\mathrm{Re} = 6000, 7000, 9000$, and 10000.

To analyze the dynamics of this process in a finite computational box, we have to keep supplying laminar flow since the turbulent region becomes longer. We resolve this
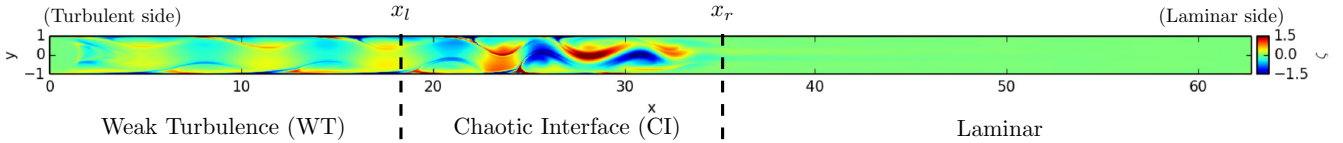
———————
[*]teramura@kyoryu.scphys.kyoto-u.ac.jp

FIG. 1. A snapshot of the vorticity deviation. ζ varies from -25 to 25 on the walls, and regions $\zeta > 1.5$ ($\zeta < -1.5$) are colored by the same color of $\zeta = 1.5$ ($\zeta = -1.5$).

problem using the damping filter [15] in the interface frame. We introduce a linear damping term into the incompressible Navier-Stokes (NS) equation to reproduce a laminar Poiseuille flow $\boldsymbol{U}_L = (1 - y^2 - c_I)\hat{\boldsymbol{x}}$ in a small region $\Omega = [0,1.4] \times [-1,1]$:

$$\frac{\partial \boldsymbol{u}}{\partial t} + (\boldsymbol{u} \cdot \boldsymbol{\nabla})\boldsymbol{u} = -\boldsymbol{\nabla} p + \frac{1}{\mathrm{Re}}\nabla^2 \boldsymbol{u} - H_{\sigma^2,\Omega}(x)(\boldsymbol{u} - \boldsymbol{U}_L),$$

$$H_{\sigma^2,\Omega}(x) = \frac{1}{\sqrt{2\pi\sigma^2}}\int_\Omega dx' \exp\left(\frac{(x-x')^2}{2\sigma^2}\right),$$

where the last term of NS equation is the damping filter term. The periodic boundary condition is imposed in the x direction. Since c_I is larger than the phase speed of the chaotic TS wave, this damping term laminarizes it, and the laminarized flow returns upstream ($x = L$) due to the periodic boundary condition. We use the stream function vorticity scheme, and thus the state variable is the z component of vorticity of the velocity deviation, $\zeta = [\boldsymbol{\nabla} \times (\boldsymbol{u} - \boldsymbol{U}_L)]_z$. We use Fourier ($x$)–Chebyshev ($y$) spectral method for spatial discretization, and explicit (convection term) and implicit (viscous term) Euler schemes for temporal evolution.

We need the following several steps to determine c_I. First, we produced a uniform turbulent state in the laboratory frame using an initial condition $u(x,y,t=0) = \varepsilon(1 - y^2)^2 \cos(kx)$ like in Ref. [13], where $\varepsilon = 0.3$ and $k = 2\pi/L$. Second, we created a turbulent puff by executing a short simulation in the laboratory frame with the damping filter $\Omega = [0,20] \cup [40,L] \times [-1,1]$. The damping filter was introduced in the laboratory frame in this step. If we execute this simulation for a long time, the entire vortices will be damped. Third, we executed a nonfiltered simulation to estimate the c_I. In this simulation the turbulent region became wider since the laminar flow is unstable, and the invading speed of the interface is about $c_I \simeq 0.8$. The turbulent region filled the systems in a short time due to the lack of the damping term, and then the interface disappeared. We could only obtain a rough estimate of the invading speed in this simulation. Last, we executed a filtered simulation on a moving frame with $c_I = 0.8$. Because 0.8 is smaller than the real value 0.855 obtained after, the interface marches slowly to the laminar side. Then we adjusted c_I for the interface not to march, and this procedure yields $c_I = 0.855$.

In this setting a turbulent-laminar interface can be simulated permanently. Figure 1 shows that the whole domain can be separated into the following three regions: weak turbulence (WT, $x \lesssim x_l$), chaotic interface (CI, $x_l \lesssim x \lesssim x_r$), and laminar ($x_r \lesssim x$) regions. Moreover, the chaotic interface contains dynamic inner structures, a meandering bulk structure, and strong wall shear layers. The weak turbulence consists of spatially modulated chaotic TS waves [11]. The separation points $x_l = 18.5$ and $x_r = 35$ are defined in the later discussion

about the energy balance and the growth of vortices near the walls.

To focus on its streamwise inhomogeneity, we consider the y-averaged energy balance equation:

$$\frac{\partial E}{\partial t} + \partial_x (J_u + J_v) = P_p + P_v - D_v + F. \tag{1}$$

The energy is defined in the interface frame: $E(x,t) = \int_{-1}^1 dy \|\boldsymbol{u}\|^2/2$. Since the walls move, there is an energy injection due to the viscosity on the walls $P_v = P_v^+ + P_v^-$, where $P_v^\pm = \mp c_I \partial_y u_x|_{y=\pm1}/\mathrm{Re}$ in addition to the bulk viscous dissipation

$$D_v = \frac{1}{\mathrm{Re}}\int_{-1}^1 dy [2(\partial_x u_x)^2 + (\partial_x u_y)^2 + (\partial_y u_x)^2]. \tag{2}$$

The term $P_p(x,t) = -\int_{-1}^1 dy(\boldsymbol{u} \cdot \boldsymbol{\nabla})p$ denotes the energy injection due to the pressure gradient and takes both positive and negative values. $P_p > 0$ means the flow accelerated by the pressure gradient, and $P_p < 0$ means the flow against the pressure gradient. P_p balances almost with the gradient of the energy flux $\partial_x J_u$, where $J_u = \int_{-1}^1 dy u_x \|\boldsymbol{u}\|^2/2$, and their spatial means are smaller than those of the viscous terms P_v and D_v. The flux due to the viscosity J_v is negligible. $F = -\int_{-1}^1 dy H_{\sigma^2,\Omega}\boldsymbol{u} \cdot (\boldsymbol{u} - \boldsymbol{U}_L)$ is the energy damping by the filter term. The left side of CI, i.e., x_l, is defined as the maximum point of the time average of J_u.

To examine the energy balance of CI, we integrate Eq. 1 over CI $[x_l, x_r]$:

$$\frac{d\bar{E}}{dt} = J_u^{(L)} - J_u^{(T)} + \bar{P}_p + \bar{P}_v - \bar{D}_v, \tag{3}$$

where the bar $\bar{\cdot}$ denotes the integral over the interface, and $J_u^{(L)} = J_u(x_r), J_u^{(T)} = J_u(x_l)$ respectively. Since the interface marches faster than the mean flow, the energy flux of the laminar flow is negative in the interface frame. In other words, the chaotic interface withdraws the energy from the laminar flow by invading it. The time averages $\langle \cdot \rangle$ of these terms are calculated over $t \in [0,300]$: $\langle J_u^{(L)} \rangle = -0.074$, $\langle J_u^{(T)} \rangle = -0.072$, $\langle \bar{P}_p \rangle = 2.4 \times 10^{-3}$, $\langle \bar{P}_v \rangle = 1.08 \times 10^{-2}$, $\langle \bar{D}_v \rangle = 1.09 \times 10^{-2}$, and the summation of them is almost zero: $\langle d\bar{E}/dt \rangle = 7.5 \times 10^{-5} \approx 0$. The time series of these values are displayed in Fig. 2. Each of these variables P_p, P_v, and $J_u^{(T)} - J_u^{(L)}$ behaves almost periodically, but their amplitudes vary chaotically. The periodicity strongly suggests the existence of a self-sustaining mechanism of the interface structure, and the chaotic amplitude suggests that its dynamics is effectively low dimensional.

Ejection-jet cycle. Here we give a concrete description of the self-sustaining mechanism of the chaotic interface. This sustaining process is constituted by the interaction among
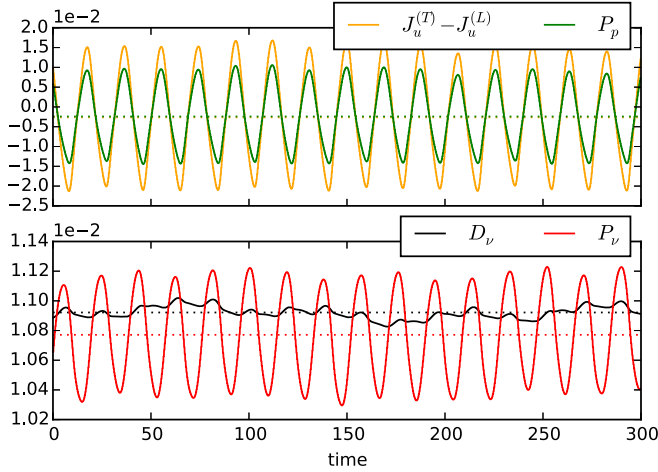
FIG. 2. Time series of each integrated value in Eq. 3. These are weakly chaotic. Dotted lines of each color denote the mean values.

FIG. 4. The vorticity at the lower wall $\zeta_L(x,t) = \zeta(x,y=-1,t)$. Black dashed line guides the minimum of $\zeta_L(x,t)$ (deep blue elongated regions) around $x \in [20:30]$. The slope of this line indicates that local minimum points move as $x_{\min} = c'_v t \simeq -0.33t$, and thus they move with $c_v = c_I - c'_v \simeq 0.52$ in the laboratory frame.

vortex ejections on the walls and the meandering jet in the bulk region. This collective dynamics is further split into four steps as summarized in Fig. 3. In step (i), a pair of sheetlike vortices is created by the meandering jet. This process takes place around $x \simeq x_r$ (see Fig. 5). In $x > x_r$ the jet becomes straight, and the creation of vortex pairs ceases.

Step (ii) is the convective growth of the vortex pair. The thin vortex pair generated in step (i) grows up into an intense vortex ejection. These vortex pairs are very thin due to the high Reynolds number Re = 8 000, and are characterized by the value of vorticity on the wall. To focus on the growth process, we use the intensity of the vorticity on the lower wall $\zeta_L(x,t) = \zeta(x,y=-1,t)$, which is displayed onto x-t plane in Fig. 4. There are elongated regions of deep blue where ζ_L takes a negative value in this x-t plot. The length of this region in the x direction is sharp enough to define the position of the vortex pair. Two dashed lines in this figure indicate that there are two traveling velocities except for c_I. The black dashed line guides the minimum of ζ_L around $x \in [20,30]$ to measure the traveling velocity c_v of the vortex pair, and this line indicates $c_v \simeq 0.52$. Since we define the velocity in the laboratory frame, positive c_v means that the vortex pair goes to the laminar side in the laboratory frame, although it moves to the turbulent side in the interface frame since $c_v - c_I < 0$. The gray dashed line indicates the traveling velocity of weak turbulence $c_w = 0.38$, which is consistent with the previous work [11].

Step (iii) is the vortex ejection process, which excites the jet and makes it meander. This ejection occurs on the turbulent side of the chaotic interface, namely around $22 < x < 28$. A very strong shear accompanies this vortex ejection process.
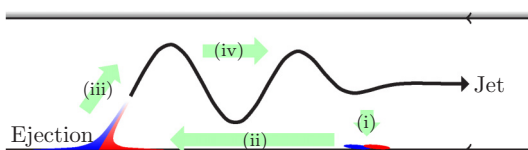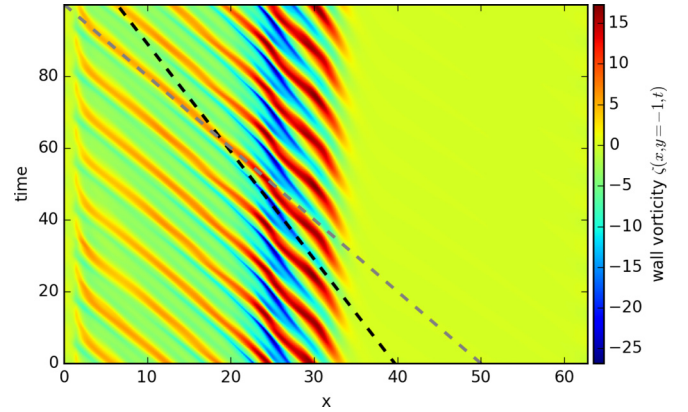
The wall unit l_τ is estimated at 2.1×10^{-3}, and the friction Reynolds number $\mathrm{Re}_\tau = l_\tau^{-1}$ is about 460. This means that the length of the interface in the x direction $(x_r - x_l)$ is 5 000 times larger than l_τ. Therefore, we should regard this interface structure as a large-scale motion in the wall-turbulence context. After the intensive ejection process, the vortex structures are swept to turbulent side, and this corresponds to the leak of the energy $\langle \Delta J_u \rangle$ from the interface to the weak turbulence region.

Step (iv) is an energy transportation taken by the meandering jet. Most part of the fluid goes to the turbulent side in the interface frame since the invading speed $c_I = 0.855$ is faster than the traveling speeds of other parts, i.e., c_w and c_v, but the meandering jet goes to the laminar side even in the interface frame. The jet is strongly meandering around the ejection $(x \sim 25)$ because of the alternate ejections on the lower and upper walls, and it becomes straight as leaving from the ejection. Then the cycle is closed, and we call this cycle an ejection-jet cycle (EJC).

To complete the EJC model, let us consider how the invading speed c_I is determined. There are two dynamical processes, the convective growth of the vortex pair and energy transportation by the jet. The spatial growth of the vortex pair on the lower wall is displayed in Fig. 5. The maximum absolute value of the vorticity ζ is realized around $x = 25$, where the intensive ejection of step (iii) occurs. The temporal minimum value of $\zeta(x,y=-1)$ changes linearly around $x \in [25,35]$ as guided by a dashed line. Since no vortex pairs exist on $x > x_r$, the end of this slope x_r defines the right boundary of CI, and its estimated value is $x_r = 35$. This linear slope should be connected with the dynamics of step (ii), but we do not have enough tools to deduce this slope. Since the vortex pair moves at the constant speed c_v in this region as shown in Fig. 4 (black dashed line), this spatial growth can be converted into a temporal growth of the minimum vorticity of the vortex pair, denoted by ω, in the Lagrangian viewpoint:

FIG. 3. A schematic view of the ejection-jet cycle.

$$\omega = -\alpha(x - x_0) = \alpha(c_v - c_I)(t - t_0), \qquad (4)$$
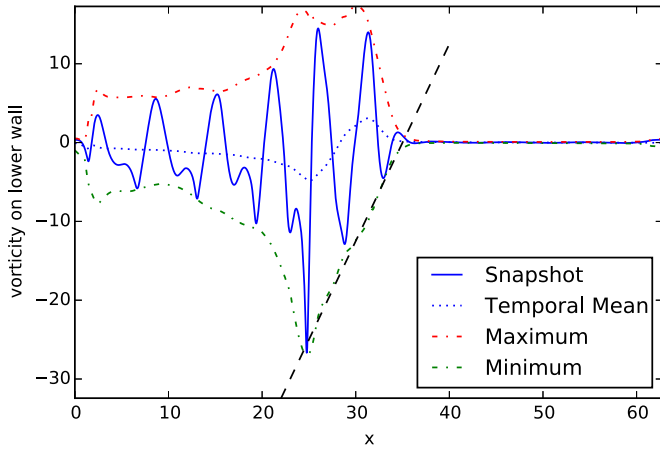
TOSHIKI TERAMURA AND SADAYOSHI TOH

FIG. 5. Spatial growth of the vorticity at the lower wall $\zeta_L(x,t) = \zeta(x, y = -1, t)$. A snapshot $\zeta_L(x, t = 58)$, temporal mean $\zeta_{\mathrm{mean}}(x) = \langle \zeta_L(x,t) \rangle_t$, maximum $\zeta_{\max}(x) = \max_{0 \leqslant t \leqslant T} \zeta_L(x,t)$, and minimum $\zeta_{\min}(x) = \min_{0 \leqslant t \leqslant T} \zeta_L(x,t)$, are displayed with $T = 100$.

where α denotes the slope in Fig. 5. In addition, we assume the minimum of the vorticity $\omega_{\min} \approx -25$, which is realized around $x = 25$ on the lower wall, is independent of c_I. It should be determined only by Reynolds number. Then Eq. 4 gives an estimate length of CI: $\Delta x = \omega_{\max}/\alpha$. The difference $c_I - c_v$ is regarded as the relative speed between the jet and the vortex pair, and thus it characterizes the mean shear exerting on the vortex pair. While the maximum velocity of the jet is faster than c_I, the typical speed of bulk structures is roughly approximated by c_I. This means that the jet loses its energy for enhancing the vortex pairs. Here we summarize the mechanism of the determination of the invading speed c_I. If c_I is too large, this energy loss prevents the creation of new vortex pairs, and thus c_I decreases. Conversely, if c_I is too small, the energy loss is suppressed, and thus the jet is accelerated. By the balance of these processes, c_I is determined spontaneously. Quantitative validations of these assumptions are left for future works.

We confirm the EJC model by removing each of the following ingredients: (a) weak turbulence, (b) vortex ejection, and (c) vortex pair excitation. Each of them is damped out by the linear damping filter. These filtered simulations help us confirm that these four steps are necessary and minimal components. A snapshot of the previous simulation is used as the initial condition of these filtered simulations. Animations visualized by the turbulent vorticity are included in the Supplemental Materials [16].

Case (a): We set $\Omega^{(a)} = [0,22] \times [-1,1]$ to damp the weak turbulent region, and to confirm the self-sustainability of the chaotic interface. In this setting we yield a permanent chaotic interface, whose invading speed and the spatial structure are hardly changed. We conclude that the following weak turbulence is additional as assumed in the EJC model. Furthermore, the selection process of c_I and the spatial structure is completely closed in the chaotic interface. In other words, the weak turbulence region hardly affects the selection process.

Case (b): We set $\Omega^{(b)} = [0,30] \times [-1,1]$ to damp the weak turbulence and the vortex ejection processes. This simulation tests whether the jet is maintained by the acceleration due to the

vortex ejection. If the meandering jet is able to sustain itself, this simulation yields a finite amplitude state in which only the meandering jet exists. The result of the simulation denies this hypothesis. The jet loses its meandering structure in a short time ($t \lesssim 20$). This simulation finally yields the laminar flow while the straightened jet remains a long time. In this sense, the meandering of the jet is only a component mechanism of this self-sustaining process, and is not self-sustaining.

Case (c): We set $\Omega^{(c)} = [30, 20\pi] \times [-1,1]$ to obstruct step (i). In this case the nonfiltered region of the chaotic interface ($20 < x < 30$) remains on the same position until $t \lesssim 20$, and then it travels to the turbulent side. This time lag corresponds to the growth time T_v of the vortex ejection, and thus this result also supports the EJC model. After a long transient period, another chaotic interface is reconstructed around $15 \lesssim x \lesssim 27$. Their invading speed and spatial structure are same as the previous one. This result insists that the chaotic interface structure is robust while a laminar region exists. This robustness is an important issue for the pattern selection problem, but the current framework of the dynamical systems approach lacks tools applicable for settling this issue.

Concluding remarks. We have investigated the turbulent-laminar interface in two-dimensional channel flow and proposed a self-sustaining mechanism, the ejection-jet cycle (EJC). From a technical viewpoint, the filtered simulation has been introduced and utilized to confirm the self-sustainability of EJC. Unlike simple interfaces such as shocks in compressible fluids, the chaotic interface (CI) has internal dynamics. It is hard to capture such dynamic properties in current approaches to interfaces. For example, there is a classical heteroclinic orbit technique [17], which has been developed to analyze effectively one-dimensional interfaces. This method rephrases the spatial structure of the interface into a heteroclinic orbit of a corresponding low-dimensional dynamical system, and thus it is incompatible with time-dependent interface. Our approach to treat the local self-sustainability directly by the filtered simulations will be an alternative approach to attack dynamical interfaces. It is well compatible with the coherent structure approach since the interface itself would be a coherent structure.

Our self-sustaining mechanism, the ejection-jet cycle (EJC), has different properties from the Waleffe's self-sustaining process (SSP) [18]. While the SSP has one spatiotemporal scale, the EJC contains two different spatial scales. These structures, namely the meandering jet and the wall vortex pair, interact by the convective growth of the vortex pair. In other words, small-scale structures are convected on a large-scale distance, and this convection makes the interaction possible. This interscale interaction mechanism is different from known ones [19]. Spatial dynamics of the interscale interaction process in isotropic turbulence, i.e., the substance of Richardson's cascade picture, is well studied in Ref. [20], where spatial convection does not play an active role. This indicates that convection-induced interscale interaction may be unique to the wall turbulence. We should try to combine such convective interaction scenario with the wall-turbulence theories, namely the mixing length picture and/or the attached eddy picture, and this remains for our future work.

Finally, we should compare our result with localized exact solutions [21–27]. Localized solutions to the Navier-Stokes

equation have been obtained in various flows at low Reynolds number. The localized dynamics corresponding to most of these exact solutions is Waleffe's SSP [28]. The existence of these solutions indicates that SSP can be embedded in laminar flow, and thus support the reaction-diffusion model of turbulent-laminar patterns [6,7]. In other words, it suggests that *reaction*, i.e., pointwise SSP dynamics, and *diffusion*, i.e., interactions among each SSP dynamics, can be separable. In the EJC model, however, the chaotic interface (CI) maintains the following weak turbulence region (WT). This one-sided relation between CI and WT is not a simple diffusion, though the dynamics of CI that appeared in the filtered simulation case (a) argued earlier can be regarded as a low-dimensional reaction. Such singular interactions among coherent structures will be important where the flux of energy and/or momentum plays critical roles, e.g., log layer in wall turbulence [8]. The EJC model could be a minimal example of this problem, and extensions to three-dimensional flows will be done in our future work.

[1] R. Venugopalan, Nucl. Phys. A **928**, 209 (2014).
[2] S. Balbus and J. Hawley, Rev. Mod. Phys. **70**, 1 (1998).
[3] U. Frisch, *Turbulence: The Legacy of AN Kolmogorov* (Cambridge University Press, Cambridge, UK, 1995).
[4] G. Kawahara, M. Uhlmann, and L. van Veen, Annu. Rev. Fluid Mech. **44**, 203 (2011).
[5] J. Jimeez and P. Moin, J. Fluid Mech. **225**, 213 (1991).
[6] D. Barkley, Phys. Rev. E **84**, 016309 (2011).
[7] P. Manneville, EPL **98**, 64001 (2012).
[8] J. Jiménez, Annu. Rev. Fluid Mech. **44**, 27 (2012).
[9] T. Ishihara, T. Gotoh, and Y. Kaneda, Annu. Rev. Fluid Mech. **41**, 165 (2009).
[10] T. Ishihara, H. Ogasawara, and J. C. Hunt, J. Fluid Struct. **53**, 50 (2014).
[11] J. Jiménez, J. Fluid Mech. **218**, 265 (1990).
[12] A. Fortin, M. Jardak, J. Gervais, and R. Pierre, J. Comput. Phys. **115**, 455 (1994).
[13] M. Umeki, Fluid Dynamics Res. **13**, 67 (1994).
[14] A. Rauh, T. Zachrau, and J. Zoller, Physica D **86**, 603 (1995).
[15] T. Teramura and S. Toh, Phys. Rev. E **89**, 052910 (2014).
[16] See Supplemental Material at http://link.aps.org/supplemental/10.1103/PhysRevE.93.041101 for the movies of simulations.
[17] W. van Saarloos, Phys. Rep. **386**, 29 (2003).
[18] J. M. Hamilton, J. Kim, and F. Waleffe, J. Fluid Mech. **287**, 317 (1995).
[19] S. Toh and T. Itano, J. Fluid Mech. **524**, 249 (2005).
[20] S. Goto, J. Fluid Mech. **605**, 355 (2008).
[21] M. Avila, F. Mellibovsky, N. Roland, and B. Hof, Phys. Rev. Lett. **110**, 224502 (2013).
[22] T. M. Schneider, D. Marinc, and B. Eckhardt, J. Fluid Mech. **646**, 441 (2010).
[23] T. M. Schneider, J. F. Gibson, and J. Burke, Phys. Rev. Lett. **104**, 104501 (2010).
[24] B. Eckhardt, J. Fluid Mech. **758**, 1 (2014).
[25] T. Khapko, T. Kreilos, P. Schlatter, Y. Duguet, B. Eckhardt, and D. S. Henningson, J. Fluid Mech. **717**, R6 (2013).
[26] S. Cherubini, P. D. Palma, J.-C. Robinet, and A. Bottaro, Phys. Fluids **23**, 51705 (2011).
[27] Y. Duguet, P. Schlatter, D. S. Henningson, and B. Eckhardt, Phys. Rev. Lett. **108**, 044501 (2012).
[28] P. Manneville, Fluid Dynamics Res. **44**, 031412 (2012).